Estimation of Regional Electrical Properties of the Heart from 12-Lead ECG and Images

Philipp Seegerer[1,2], Tommaso Mansi[1], Marie-Pierre Jolly[1], Dominik Neumann[1,2], Bogdan Georgescu[1], Ali Kamen[1], Elham Kayvanpour[3], Ali Amr[3], Farbod Sedaghat-Hamedani[3], Jan Haas[3], Hugo Katus[3], Benjamin Meder[3], and Dorin Comaniciu[1]

[1] Imaging and Computer Vision, Siemens Corporate Technology, Princeton, NJ, USA
[2] Pattern Recognition Lab, FAU Erlangen-Nürnberg, Germany
[3] Department of Internal Medicine III, University Hospital Heidelberg, Germany

Abstract. Computational models of cardiac electrophysiology are being investigated for improved patient selection and planning of therapies like cardiac resynchronization therapy (CRT). However, their clinical applicability is limited unless their parameters are fitted to the physiology of an individual patient. In this paper, a method that estimates spatially-varying electrical diffusivities from routine ECG data and dynamic cardiac images is presented. Contrary to current methods based on invasive electrophysiology studies or body surface potential mapping, our approach relies on widely available 12-lead ECG and motion information obtained from clinical images. First, a map of mechanical activation time is derived from a cardiac strain map. Then, regional electrical diffusivities are personalized such that the computed cardiac depolarization matches both the mechanical activation map and measured ECG features. The fit between measured and computed electrocardiography data after model personalization is evaluated on 14 dilated cardiomyopathy patients, exhibiting low mean errors in terms of the diagnostic ECG features QRS duration (0.1 ms) and electrical axis (10.6°). The proposed regional approach outperforms global personalization when 12-lead ECG is the only electrophysiology data available. Furthermore, promising results of a preliminary CRT study on one patient demonstrate the predictive power of the personalized model.

1 Introduction

Heart failure (HF) is a major cause of death in the western world (4-year survival rate of 50% [1]). Approximately 25% of HF patients are affected by a left bundle branch block, an obstruction in the cardiac conduction pathway, which decreases the speed of the electrical wave in the left ventricle [2]. Irregular mechanical activation of the myocardium is among its consequences. For patients with a prolonged QRS complex (QRS $\geq$ 120 ms) and low left ventricular ejection fraction, cardiac resynchronization therapy (CRT) is a well-established treatment [3]. CRT consists in implanting electrodes into the heart to pace the myocardium artificially and "resynchronize" cardiac contraction. However, 25-30% of patients do not respond to CRT. Hence, more adequate patient selection

and therapy planning is required [3]. Combining medical imaging with computational modeling of the heart could provide new tools towards this goal.

To that end, computational models of cardiac electrophysiology (EP) are being investigated. Recent developments enable fast EP computation when coupled with phenomenological models of the cardiac action potential [4, 5]. However, model personalization, i. e. adjusting model parameters so that the model output fits clinical data of an individual patient, is a *sine qua non* for clinical applicability. Comprehensive and spatially-dense EP information can be gathered by invasive endocardial mapping or body surface potential mapping [6, 7]. However, these measurements are often not available for diagnosis or disease monitoring purposes. Therefore, methods of personalizing EP models from routinely acquired 12-lead ECG have been proposed recently [8]. Due to the sparsity of the data, these approaches focus on the estimation of global parameters (one diffusion value per ventricle). As a consequence, complex pathologies like localized bundle branch blocks cannot be captured precisely.

Evidence is growing that irregularities in mechanical activation are related to abnormal electrical activation [9] and that indicators derived from such irregularities may be predictive for CRT outcome [10]. In order to measure mechanical activation, methods for quantifying myocardial strain from magnetic resonance images (MRI) have been developed [11]. The basic concept is to track the myocardium over time and compute the strain tensor from the estimated deformation field. This information can be used to estimate electrical activation patterns non-invasively [12].

In this paper, a method that estimates spatially-varying electrical diffusivity from ECG and strain maps is presented. While ECG provides global information of cardiac electrophysiology, strain maps are used to identify regional abnormalities. Mechanical myocardial activation is computed to identify the location of a block in the conduction system. Then, electrical diffusivity is estimated such that calculated ECG features match the measurements while the electrical depolarization pattern respects the block. The method is evaluated on 14 dilated cardiomyopathy patients, showing a significant improvement over global fitting in terms of goodness of fit between measured and simulated ECG features. Furthermore, the predictive power of the model is evaluated on one patient who underwent CRT, where better prediction accuracy is observed when using the proposed regional personalization compared to the global method.

2 Method

The workflow of our method is illustrated in Fig. 1. A mechanical activation map of the left ventricular myocardium is derived from Cine MRI, from which a line of block is localized (Sec. 2.1). The images are further used to create an anatomical heart model. Cardiac EP is calculated and the electrical potential propagated to the torso, where 12-lead ECG tracing is derived (Sec. 2.2). Eventually, the model parameters are personalized within a non-linear inverse optimization framework using clinically measured ECG data and the block information (Sec. 2.3).

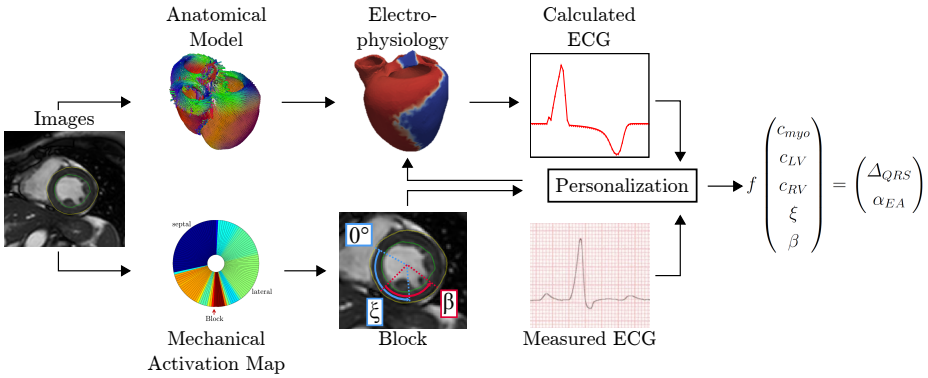

Fig. 1. Workflow of proposed cardiac electrophysiology personalization framework.

2.1 Computation of Mechanical Activation Time

Mechanical activation time maps of the left ventricle (LV) are computed from short axis Cine MRI in four steps: *i)* left ventricular myocardium segmentation, *ii)* 2-D, slice-based myocardium tracking, *iii)* strain computation and *iv)* mechanical activation map calculation, as described below.

Myocardium Segmentation The LV volume is automatically segmented on the 2-D slices using a 2-D+time algorithm [13]. First, the LV blood pool is automatically localized using temporal Fourier transform and isoperimetric clustering to find the most compact and circular bright moving object in the slices. Then, the myocardium boundaries are extracted using a shortest path algorithm in polar space. Temporal consistency is enforced by the backward and forward fields of an inverse consistent deformable registration. For each slice, all frames are registered to a reference frame at end-diastole. Contour sets are generated by successively segmenting each frame and propagating the contours to all the other frames. The best contour set is chosen as the final segmentation.

Myocardium Tracking Deformable image registration is performed using an inverse consistent diffeomorphic algorithm [14]. The registration computes a dense deformation field between any two frames in a slice without having to register every possible pair of frames explicitly. To that end, the inverse consistency of the registration is exploited. The deformation field between frames f_j and f_k is obtained by compounding the deformation field between frame f_k and f_1 at end-diastole and the inverse deformation field between frames f_j and f_1. All frames f_i are registered to f_1 yielding the deformation fields Φ_i.

Strain Computation The Lagrangian strain tensor E is derived from Φ_i according to $E = 1/2(\nabla\Phi_i + \nabla\Phi_i^T + \nabla\Phi_i\nabla\Phi_i^T)$. Computing the norm of the principal strain (eigenvectors of E) with the largest eigenvalue for every myocardium pixel in every frame yields a spatially and temporally resolved map of LV strain. Basal and apical slices are excluded from the subsequent analysis due to insufficient image quality.

Mechanical Activation Map Afterwards, a polar map of mechanical activation is computed from the strain maps. More precisely, the LV is represented as a circle divided into 120 circumferential segments (Fig. 3, right panel). For each segment the strain is averaged across the myocardium. A polar strain map is computed for each time frame. Then, the time to peak of principal strain is identified per segment as the time of mechanical activation. Finally, median filtering is applied to remove outliers due to noise.

In a subject without block in the conduction system, the mechanical activation propagates uniformly from the septum to the lateral wall, i. e. the latest activated segment is at the lateral wall. However, if there is a block in the conduction system, the latest activated segment is shifted towards the septum, i. e. the myocardium does not contract uniformly. As shown in Fig. 1 ("Block"), the position of the line of block in the myocardium is described by an circumferential angle ξ (with respect to the long axis of the heart). The extent of the block is defined by an angle β. A voxel is considered to be inside the block if its circumferential angle is in a certain range Ω around ξ. In our experiments, we set $\Omega = [\xi - 0.5\beta; \xi + 0.5\beta]$.

2.2 Forward Model of Cardiac Electrophysiology

A fast cardiac electrophysiology model based on the lattice Boltzmann method is employed [4]. First, the heart is segmented automatically from MRI images by a data-guided machine learning algorithm [15]. A rule-based model of myocardial fiber architecture (fiber angles vary linearly from epi- to endocardium: from -40° to 65° [16]) is calculated in order to take anisotropy into account. This can be advanced without any modification by using fiber atlases (a sensitivity analysis is ongoing). Trans-membrane potentials are calculated according to the Mitchell-Schaeffer model [17], which is solved efficiently using the LBM-EP method [4].

The conduction velocity is governed by electrical diffusion parameters. Three domains with different diffusivities c are considered in the model, as pictured in Fig. 2: the slow-conducting myocardium (c_{myo}) and the fast-conducting left and right ventricular endocardia (c_{LV} and c_{RV}). Afterwards, the potentials are mapped to a torso atlas using the boundary element method [4], and the 12-lead ECG is calculated. Therefrom, important clinical ECG features, namely the duration of the QRS complex Δ_{QRS} and the electrical axis α_{EA}, are derived automatically.

2.3 Electrical Diffusivity Estimation

If the mechanical activation map shows an irregular pattern, i. e. the location of the latest contraction is significantly moved towards the septum, a block in the conduction system is considered and defined as a new domain in the EP model. Its position and extent are described by two angles ξ and β (Sec. 2.1). The diffusivity of the endocardial tissue inside the block region is set to the low myocardial diffusivity c_{myo} because the electrical wave propagates over the myocytes if the conduction pathways are obstructed.

Algorithm 1 Regional EP Personalization

Require: Initial diffusivity $c_{myo}^{init}, c_{LV}^{init}, c_{RV}^{init}$ and block parameters ξ^{init}, β^{init}

1: $\kappa^0 = \arg\min_\kappa d_{QRS}\left(\kappa \cdot (c_{myo}^{init}, c_{LV}^{init}, c_{RV}^{init})\right)$
2: $(c_{myo}^0, c_{LV}^0, c_{RV}^0) = \kappa^0 \cdot (c_{myo}^{init}, c_{LV}^{init}, c_{RV}^{init})$
3: **for** $i = 1$ **to** $i = N$ **do**
4: $\quad (c_{LV}^{i*}, c_{RV}^{i*}, \xi^i) = \arg\min_{c_{LV}, c_{RV}, \xi} (\lambda \cdot d_{QRS}(c_{LV}, c_{RV}, \xi) + d_{EA}(c_{LV}, c_{RV}, \xi))$
5: $\quad \beta^i = \arg\min_\beta (\lambda \cdot d_{QRS}(\beta) + d_{EA}(\beta))$
6: $\quad \kappa^i = \arg\min_\kappa d_{QRS}\left(c_{myo}^{i-1}, c_{LV}^{i*}, c_{RV}^{i*}\right)$
7: $\quad (c_{myo}^i, c_{LV}^i, c_{RV}^i) = \kappa^i \cdot (c_{myo}^{i-1}, c_{LV}^{i-1}, c_{RV}^{i-1})$
8: **end for**
9: **return** Personalized EP parameters c_{myo}^N, c_{LV}^N, c_{RV}^N, ξ^N, β^N

The block region enables regional manipulation of the electrical wave propagation by targeted deceleration. The block position is estimated from the mechanical activation maps (Sec. 2.1). Then, the diffusivities c_{myo}, c_{LV} and c_{RV} and the block parameters ξ and β are personalized such that the calculated ECG features match the measurements $\Delta_{QRS,m}$ and $\alpha_{EA,m}$. This is achieved by nonlinear inverse optimization using BOBYQA, a robust gradient-free optimization technique [18]. First, a factor κ for the diffusivities c is optimized, as in [8]. Secondly, c_{LV}, c_{RV} and ξ are optimized. Thereby, ξ is refined inside a range of $\pm 45°$ around the position estimated from the mechanical activation maps to cope with inaccuracies in block localization. The diffusivity of the block region stays equal to c_{myo}. In the next steps, β and κ are optimized. These three steps are iterated (convergence typically after $N = 3$ iterations). The errors of the calculated ECG features are described by $d_{QRS}(\Psi) = (\Delta_{QRS,m} - \Delta_{QRS}(\Psi))^2$ and $d_{EA}(\Psi) = (\alpha_{EA,m} - \alpha_{EA}(\Psi))^2$, where Ψ denotes model input parameters. The weighting factor λ is chosen to cope with distinct units. All optimization steps ($\arg\min$) are initialized with the previously estimated parameters. The personalization workflow is sketched in Algorithm 1.

3 Experiment and Results

Experimental Setup For experimentation, 14 dilated cardiomyopathy (DCM) patients who showed irregular contraction patterns in the estimated mechanical activation maps were selected. Tracked myocardium contours are presented in Fig. 2, right panel. The temporal changes in principal strain of an example sector of one patient are shown in Fig. 3, left panel. Fig. 3, right panel illustrates the mechanical activation map computed from the Cine MRI for a patient with block in the conduction system.

Personalization Performance EP model personalization with the proposed regional approach was compared against a global state-of-the-art method that relies on 12-lead ECG only, similar as in [8]. The proposed approach differs from the global method only by the incorporation of the block (Algorithm 1, Lines 4

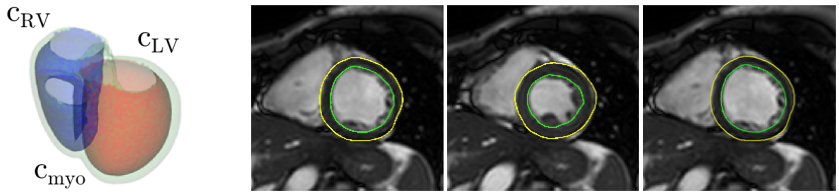

Fig. 2. *Left Panel:* Electrophysiology domains. *Right Panel:* Tracked endo- and epicardial contours (left ventricle) over time, showing good agreement to the image data.

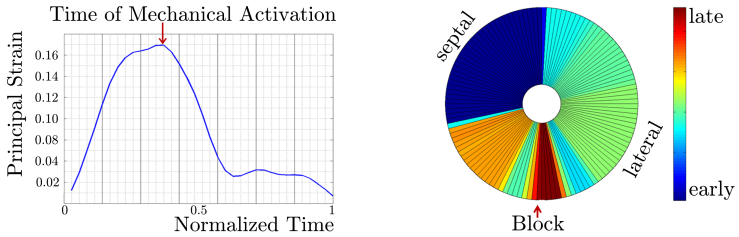

Fig. 3. *Left panel*: Principal strain of an example segment over time. The time of the peak is assumed to signify mechanical activation. *Right panel*: Polar map of mechanical activation (LV) with irregular contraction pattern and identified block location.

and 5). The output of the personalized models was compared to clinical measurements. Clinically plausible acceptance ranges were defined for both ECG features: $\varepsilon_{QRS} < 10\,\text{ms}$ and $\varepsilon_{EA} < 20°$. Both approaches captured Δ_{QRS} well with maximum errors of less than 1 ms. The average error of our method for α_{EA} was $10.6° \pm 20.0°$, which is well within the acceptance range. Using the global method, the average error was about twice as large: $21.9° \pm 33.8°$. In Tab. 1, the computed α_{EA} of both methods are compared to the measurements for each individual patient. According to the acceptance criteria defined above, α_{EA} was matched for 11 patients using our regional approach and only for 10 patients using the global approach. As a conclusion, the proposed regional approach can significantly improve EP model personalization over state-of-the-art global methods in terms of goodness of fit between measured and simulated ECG features.

Predictive Power After fitting the model to preoperative data using the proposed regional approach on the one hand, and the global approach on the other hand, CRT lead placement and programming were mimicked *in silico* for an LV and an RV pacing scenario on the employed model in order to evaluate its predictive power. The experiments were conducted on one CRT patient (Patient 14, Tab. 1), for whom pre- and postoperative ECG data were available. The outcome was compared to the postoperative measurements $(\Delta_{QRS,post}, \alpha_{EA,post})$: $(149\,\text{ms}, -13°)$ and $(176\,\text{ms}, -40°)$ for LV and RV pacing, respectively. Results show that while QRS prediction performs similarly well for both personaliza-

Table 1. Measured and computed electrical axis (in degrees) using our approach ("Regional") and a state-of-the-art approach ("Global"), see text for details. Values that are outside of the acceptance ranges are highlighted in bold print.

Patient	Measured	Regional	Global	Patient	Measured	Regional	Global
1	-99	**-63**	-99	8	57	57	56
2	-3	-6	-3	9	90	89	**-172**
3	-40	-42	-40	10	-17	**22**	**24**
4	112	112	112	11	21	21	19
5	-15	-15	-15	12	45	45	26
6	32	**-31**	**-39**	13	60	60	**-9**
7	-12	-12	-12	14	-12	-16	-16

tion methods and both pacing scenarios, for LV pacing the regional method ($147\,\mathrm{ms}, -25°$) predicted the change in electrical axis better, meeting the defined acceptance criteria, while the global method ($149\,\mathrm{ms}, -54°$) failed. RV pacing predictions were similar for both personalized models, as only the left ventricle is affected by the block estimation with little impact in RV pacing scenarios. The regional method predicted ($177\,\mathrm{ms}, -52°$) and the global method ($175\,\mathrm{ms}, -50°$), both well within the defined acceptance ranges. This preliminary CRT study suggests that our personalization framework could improve the ability of the model to predict CRT outcomes, which is an important result towards clinical applicability of computational cardiac models.

4 Discussion and Conclusion

This work presents a novel method to estimate regional electrical diffusivity from dynamic cardiac images and 12-lead ECG. The underlying assumption is that abnormalities in mechanical activation time are related to conduction system failure. Thus, we incorporated that knowledge in a gradient-free estimation framework. It can be used with any electrophysiology model or solver. Furthermore, our approach relies on data that is acquired non-invasively and is widely available, in contrast to other state-of-the-art methods. Results on 14 DCM patients showed that our approach achieves promising goodness of fit between measured and calculated ECG features. However, the personalization fails on 3 cases due to mismatched electrical axis. This could be caused by imprecise ECG lead positioning or the presence of complex pathologies which the model is not capable to capture. Hence, the next step will be to include further regionality in the personalization to allow the model to adapt to a larger variety of pathologies. Furthermore, the predictive power of the model will be evaluated more extensively in the future as soon as additional CRT cases are at our disposal. Moreover, fiber architecture can be modeled close to the real physiology once in vivo diffusion tensor imaging (DTI) data are available.

References

1. Dickstein, K., Cohen-Solal, A., Filippatos, G., McMurray, J.J., Ponikowski, P., Poole-Wilson, P.A., Strömberg, A., Veldhuisen, D.J., Atar, D., Hoes, A.W., et al.: Esc guidelines for the diagnosis and treatment of acute and chronic heart failure. European journal of heart failure **10**(10) (2008) 933–989
2. Zannad, F., Huvelle, E., Dickstein, K., Veldhuisen, D.J., Stellbrink, C., Kber, L., Lechat, P.: Left bundle branch block as a risk factor for progression to heart failure. European journal of heart failure (2007)
3. Kass, D.A.: Cardiac resynchronization therapy. Journal of cardiovascular electrophysiology **16**(s1) (2005) 35–41
4. Zettinig, O., Mansi, T., Neumann, D., Georgescu, B., Rapaka, S., Seegerer, P., Kayvanpour, E., Sedaghat-Hamedani, F., Amr, A., Haas, J., Steen, H., Katus, H., Meder, B., Navab, N., Kamen, A., Comaniciu, D.: Data-driven estimation of cardiac electrical diffusivity from 12-lead ECG signals. Medical Image Analysis (2014)
5. Talbot, H., Duriez, C., Courtecuisse, H., Relan, J., Sermesant, M., Cotin, S., Delingette, H.: Towards real-time computation of cardiac electrophysiology for training simulator. In: STACOM. Springer (2013) 298–306
6. Relan, J., Chinchapatnam, P., Sermesant, M., Rhode, K., Ginks, M., Delingette, H., Rinaldi, C.A., Razavi, R., Ayache, N.: Coupled personalization of cardiac electrophysiology models for prediction of ischaemic ventricular tachycardia. Interface Focus **1**(3) (2011) 396–407
7. Dössel, O., Krueger, M.W., Weber, F.M., Wilhelms, M., Seemann, G.: Computational modeling of the human atrial anatomy and electrophysiology. Medical & biological engineering & computing **50**(8) (2012) 773–799
8. Neumann, D., Mansi, T., Grbic, S., Voigt, I., Georgescu, B., Kayvanpour, E., Amr, A., Sedaghat-Hamedani, F., Haas, J., Meder, B., Katus, H., Hornegger, J., Kamen, A., Comaniciu, D.: Automatic image-to-model framework for patient-specific electromechanical modeling of the heart. In: ISBI, IEEE (2014)
9. Risum, N., Strauss, D., Sogaard, P., Loring, Z., Hansen, T.F., Bruun, N.E., Wagner, G., Kisslo, J.: Left bundle-branch block: The relationship between electrocardiogram electrical activation and echocardiography mechanical contraction. American heart journal **166**(2) (2013) 340–348
10. Jackson, T., Sohal, M., Chen, Z., Child, N., Sammut, E., Behar, J., Claridge, S., Carr-White, G., Razavi, R., Rinaldi, C.A.: A u-shaped 'type ii' contraction pattern in patients with strict left bundle branch block predicts super-response to cardiac resynchronization therapy. Heart Rhythm (2014)
11. Oubel, E., De Craene, M., Hero, A.O., Pourmorteza, A., Huguet, M., Avegliano, G., Bijnens, B., Frangi, A.F.: Cardiac motion estimation by joint alignment of tagged mri sequences. Medical Image Analysis **16**(1) (2012) 339–350
12. Prakosa, A., Sermesant, M., Allain, P., Villain, N., Rinaldi, C., Rhode, K., Razavi, R., Delingette, H., Ayache, N.: Cardiac electrophysiological activation pattern estimation from images using a patient-specific database of synthetic image sequences. IEEE Transactions on Biomedical Engineering **61**(2) (2014) 235–245
13. Jolly, M.P., Guetter, C., Guehring, J.: Cardiac segmentation in mr cine data using inverse consistent deformable registration. In: ISBI, IEEE (2010) 484–487
14. Guetter, C., Xue, H., Chefd'Hotel, C., Guehring, J.: Efficient symmetric and inverse-consistent deformable registration through interleaved optimization. In: ISBI, IEEE (2011) 590–593

15. Zheng, Y., Barbu, A., Georgescu, B., Scheuering, M., Comaniciu, D.: Four-chamber heart modeling and automatic segmentation for 3-d cardiac ct volumes using marginal space learning and steerable features. IEEE T-MI **27**(11) (2008) 1668–1681
16. Lombaert, H., Peyrat, J., Croisille, P., Rapacchi, S., Fanton, L., Cheriet, F., Clarysse, P., Magnin, I., Delingette, H., Ayache, N.: Human atlas of the cardiac fiber architecture: Study on a healthy population. IEEE T-MI **31**(7) (2012) 1436–1447
17. Mitchell, C.C., Schaeffer, D.G.: A two-current model for the dynamics of cardiac membrane. Bulletin of mathematical biology **65**(5) (2003) 767–793
18. Powell, M.J.: The bobyqa algorithm for bound constrained optimization without derivatives. Cambridge NA Report, University of Cambridge, Cambridge (2009)